Theor Chem Account (2008) 121:109–122
DOI 10.1007/s00214-008-0454-3

REGULAR ARTICLE

End-substitution effect on the geometry and electronic structure of oligoheterocyclics

Gui-Ling Zhang · Hui Zhang · Dong-Ping Li · Dan Chen · Xiao-Yang Yu · Bo Liu · Ze-Sheng Li

Received: 13 February 2008 / Accepted: 30 April 2008 / Published online: 11 June 2008
© Springer-Verlag 2008

Abstract The end-substitution effects on the geometric and electronic structures of oligoheterocyclics are systematically studied using the density functional theory. It is found that the influence of the end-substitution does not depend on the heteroatom. End-substitution plays a fine-tune effect on the geometry and the excitation state. While the influences on the conducting type (p-type or n-type) and the inter-chain charge carrier hoping channels are much different between the electron-donating $–CH_3$ and electron–accepting –CN substitutions. Both molecular electrostatic potentials and charge carrier injection rates indicate that the $–CH_3/–CH_3$ substitution is beneficial to the p-type doping, while the –CN/–CN substitution is in favor of the n-type doping, which is in agreement with the experimental observations. The $–CH_3$ substituted packing dimers exert similar intermolecular interactions to the unsubstituted ones. The –CN substituted packing dimers yield much stronger intermolecular interactions comparing to the $–CH_3$ substituted ones. It could be anticipated that the –CN substitution would be helpful to the charge carrier hopings between chains and thereby enhance the conductivity.

Keywords Oligoheterocyclics · End-substitution · Theoretical calculation

1 Introduction

Five-membered oligoheterocyclics such as oligothiophene, oligofuran, and oligopyrrole have raised an extensive interest in the last decade because they display fascinating semiconductivity, photoconductivity and electroluminescence, etc. [1,2]. Many efforts toward improving functions of these materials are underway by introducing proper designed substituents [3–12], a noticeable case is the end-substitution [13–19]. Many experimentalist have devoted to the synthesis of end-substituted oligothiophenes for different purpose, such as for enhancing chemical stability [20,21], designing self-assembly function [22], and achieving n-type conductivity [23–28], etc. In recent years, theoretical works have revealed that polycyclopentadiene, polysilole, and polyphosphole are good candidates for exploring narrow band gap conducting materials [29–31]. In experiments, oligosiloles [32–40] and oligophospholes [41–46] have already been successfully synthesized. To the best of our knowledge, the end-substitution effects on the geometric and electronic structures of these homologous compounds are seldom systematically discussed. Theoretical investigations on a series of end-substituted oligoheterocycles are thereby desirable for designing novel functional materials, which is the main purpose of this work.

Various theoretical calculations were performed on the end-substituted oligothiophenes [47–54], most of which have mainly concentrated on the analysis of the end-substitution effects on geometries and HOMO–LUMO gaps of single oligothiophene chains. In experiments, it is found that the fabrication of ambipolar transistors or devices based on p–n heterojunctions is mainly dependent on the switch between

Electronic supplementary material The online version of this article (doi:10.1007/s00214-008-0454-3) contains supplementary material, which is available to authorized users.

G.-L. Zhang · H. Zhang · D.-P. Li · D. Chen · X.-Y. Yu · B. Liu (✉)
College of Chemical and Environmental Engineering,
Harbin University of Science and Technology,
Harbin 150080, People's Republic of China
e-mail: hust_zhanghui1@hotmail.com

Z.-S. Li
Institute of Theoretical Chemistry, State Key Laboratory
of Theoretical and Computational Chemistry,
Jilin University, Changchun 130023,
People's Republic of China

p-type and n-type conductivity tuned by substituents [23–28]. However, for a series of oligoheterocycles, influences of the end-substitutions on the conductive types are seldom theoretically discussed. Another challenging task for both experimental and theoretical works is to try to investigate the inter-chain interactions [55–64], which is of particular importance for surveying charge carrier hoping channels between chains. To probe the charge carrier hoping channels induced by substituents is still desirable. For example, experiments [65,66] have revealed that the formation of the inter-chain C≡N · · · H hydrogen bonds in –CN substituted oligothiophene films could enhance the conductivity, while other charge carrier hoping channels such as C ≡ N · · · π and C ≡ N · · · N ≡ C interactions are seldom considered.

In this paper, electron-donating –CH_3 group and electron-withdrawing –CN group are selected as the end-substituents. We firstly investigate the end-substitution effects on the geometric and electronic structures for a series of heterocycle trimers (cf. Fig. 1), and then we look into the inter-chain charge carrier hoping channels induced by end-substituents for some designed packing dimers (cf. Fig. 2).

The following symbols are used for the discussions below (Fig. 1): H − π − H for $R_1 = R_2 = -$H unsubstituted molecules; $CH_3-\pi-CH_3$ for $R_1 = R_2 = -CH_3$ substituted molecules; $CH_3 - \pi - CN$ for $R_1 = -CH_3$ and $R_2 = -CN$ substituted molecules; $CN - \pi - CN$ for $R_1 = R_2 = -CN$ substituted molecules; $-CH_3/-CH_3$ for $R_1 = R_2 = -CH_3$ substitution; $-CH_3/-CN$ for $R_1 = -CH_3$ and $R_2 = -CN$ substitution; and $-CN/-CN$ for $R_1 = R_2 = -CN$ substitution.

2 Theoretical method

Density functional theory (DFT) [67] as implemented in Gaussian03 program [68] has been employed to optimize the geometries of **a**–**f**. In our previous works, the B3LYP [69] functional and 6-31G* basis set were validated to be reasonable for describing oligoheterocyclics [70–72]. So, the B3LYP functional and 6-31G* basis set are still employed in this paper.

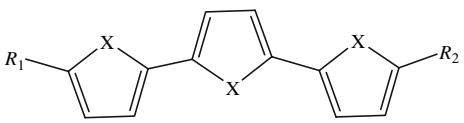

a	X=CH_2	**b**	X=NH	**c**	X=O
1a	R_1=R_2=-H	**1b**	R_1=R_2=-H	**1c**	R_1=R_2=-H
2a	R_1=R_2=-CH_3	**2b**	R_1=R_2=-CH_3	**2c**	R_1=R_2=-CH_3
3a	R_1=-CH_3, R_2=-CN	**3b**	R_1=-CH_3, R_2=-CN	**3c**	R_1=-CH_3, R_2=-CN
4a	R_1=R_2=-CN	**4b**	R_1=R_2=-CN	**4c**	R_1=R_2=-CN
d	X=SiH_2	**e**	X=PH	**f**	X=S
1d	R_1=R_2=-H	**1e**	R_1=R_2=-H	**1f**	R_1=R_2=-H
2d	R_1=R_2=-CH_3	**2e**	R_1=R_2=-CH_3	**2f**	R_1=R_2=-CH_3
3d	R_1=-CH_3, R_2=-CN	**3e**	R_1=-CH_3, R_2=-CN	**3f**	R_1=-CH_3, R_2=-CN
4d	R_1=R_2=-CN	**4e**	R_1=R_2=-CN	**4f**	R_1=R_2=-CN

Fig. 1 The selected compounds for studying the substitution effect on single oligoheterocyclics

The time-dependent density functional theory (TDDFT) [73,74] is employed to calculate the optical properties on the basis of B3LYP/6-31G* optimized geometries. Ten lowest excitation states of each compound are computed, from which the excitation spectra was theoretically simulated with a Gaussian broadening of 0.6 eV of Full Width Half Maximun.

The natural bond orbital (NBO) analysis [75–78] was performed based on the B3LYP/6-31G* optimized geometries to quantitatively evaluate the interaction energy between electron donors and acceptors.

Molecular electrostatic potentials [79–81] were computed to examine the substitution effect on the charge density distributions. Molecular electrostatic potentials of all structures were calculated at the B3LYP/6-31G* optimized geometries and plotted using gOpenMol 2.32 [82,83].

The topological properties for investigating the inter-chain hoping channels of charge carriers for model packing dimers $\mathbf{a}_{1-11}$, $\mathbf{b}_{1-11}$, and $\mathbf{c}_{1-11}$ were examined by using the atoms in molecules methodology (AIM) [84,85] with the AIM2000 program package [86].

3 Results and discussion

In this section we will discuss the end-substitution effect on the geometric and electronic structures of single trimers, **a**–**f**, in Fig. 1. Then we try to analyze the inter-chain charge carrier hoping channels of some designed packing dimers induced by the substituents, R.

3.1 Effect on geometry

An important factor related to the extent of the π conjugation is the chain planarity which can be reflected by the tortional angle θ as defined in Scheme 1. $\theta = 0°$ and $\theta = 180°$ correspond to *anti* and *syn* conformations, respectively. The data of the average $\overline{\theta}$ for **a**–**f** obtained from B3LYP/6-31G* optimizations are listed in Table 1. The planar *anti* structure is not changed after –CH_3 and –CN substitutions because all the values of $\overline{\theta}$ are near zero (<2.2°). This calculated result is in agreement with the experimental observations for the substituted oligothiophenes [11,20,21,66,87,88].

Another important parameter of interested with respect to the π conjugation is the bond alternation parameter, δ, defined here as the bond length difference between two adjacent single and double bonds. Small δ value may correspond to good π conjugation. Here, two bond alternation parameters, δ_{intra} and δ_{inter}, are defined as $\delta_{\text{intra}} = r_{\beta\beta} - r_{\alpha\beta}$ and $\delta_{\text{inter}} = r_{\alpha\alpha} - r_{\alpha\beta}$, where $r_{\alpha\beta}$ and $r_{\beta\beta}$ are the intra-ring

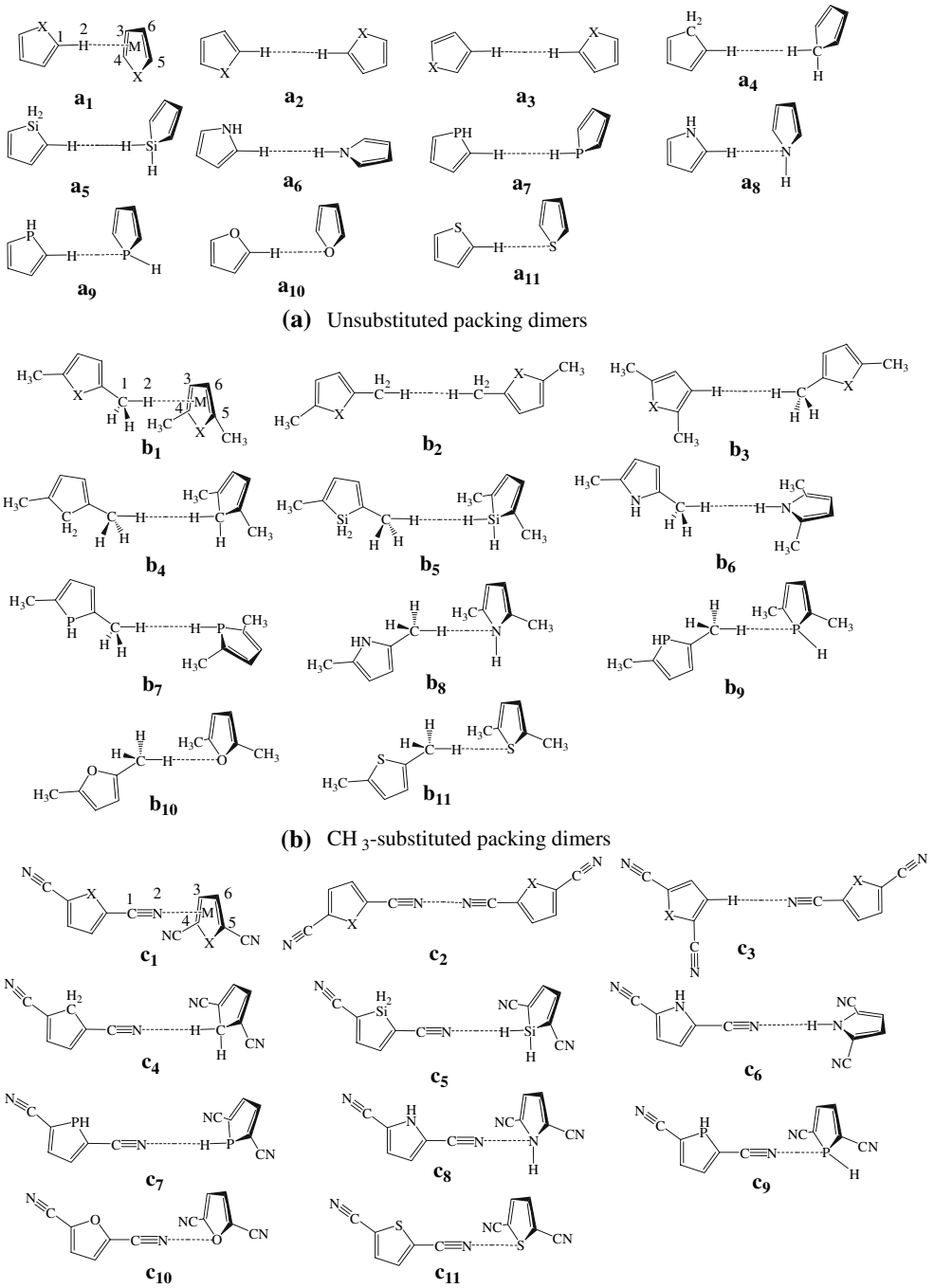

Fig. 2 The selected model packing dimers for AIM calculations. X are the heteroatoms: CH_2, NH, O, SiH_2, PH, and S. The atoms of the substituent of one ring used to interact with another ring are labeled as 1 and 2, and the carbon atoms of another ring are labeled as 3, 4, 5, and 6 as given in $\mathbf{a}_1$, $\mathbf{b}_1$, and $\mathbf{c}_1$. In dimers $\mathbf{a}_1$, $\mathbf{b}_1$, and $\mathbf{c}_1$, the line C_3C_5 intersects the line C_4C_6 at M

bond length, and $r_{\alpha\alpha}$ denotes the inter-ring bond length as being labeled in Scheme 1. The average intra- and inter-ring bond alternation parameters, $\bar{\delta}_{\text{intra}}$ and $\bar{\delta}_{\text{inter}}$, are listed in Table 1. By comparing with the parent molecules, the replacement of two terminal hydrogen atoms by two donor $-CH_3$ groups (CH_3–π–CH_3) exerts little influence on both

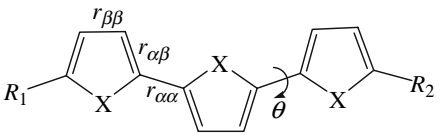

X=CH_2, NH, O, SiH_2, PH, S

$\delta_{intra}=r_{\beta\beta}-r_{\alpha\beta}$ $\delta_{inter}=r_{\alpha\alpha}-r_{\alpha\beta}$

$\theta=0^\circ$: *anti* conformer; $\theta=180^\circ$: *syn* conformer

Scheme 1 Torsion angle and bond alternation parameter

intra- and inter-ring bond alternations with the decrease of $\bar{\delta}_{\text{intra}}$ and $\bar{\delta}_{\text{inter}}$ being only in the range of 0.0–0.002 Å. In experiments, it has been also found that the introduction of two –CH_3 groups at end-positions in quaterthiophene does not affect the molecular and crystal structure related to the unsubstituted system [66]. The presence of the donor –CH_3 group on one end and the accepter –CN group on another (CH_3–π–CN) could lead to decreases of 0.007–0.009 Å and 0.004–0.005 Å for $\bar{\delta}_{\text{intra}}$ and $\bar{\delta}_{\text{inter}}$, respectively. The electron-withdrawing –CN/–CN substitution (CN–π–CN) lowers the values of $\bar{\delta}_{\text{intra}}$ and $\bar{\delta}_{\text{inter}}$ by 0.011–0.012 and 0.004–0.005 Å, respectively. Therefore, the attachment of –CH_3/–CN or –CN/–CN can enhance both aromatic and quinoid characters of the carbon skeleton. In contrast, –CH_3/–CH_3 substitution yields little influence on the bond alternation. It seems that more –CN groups result in more decrease of the bond alternation, i.e., $\bar{\delta}$ values are ordered as CH_3–π–CH_3 > CH_3–π–CN > CN–π–CN. Previous work [71,72] suggested that small bond length alternation may correspond to narrow HOMO–LUMO gap, Δ, and low TDDFT excitation energy, E_g. This correlation is suitable for most calculated results except some special cases in **b** and **c** (cf. Table 1, Fig. 3). For example, **3b** > **4b** for $\bar{\delta}$, but the inverse is true for Δ and E_g (**3b** < **4b**).

3.2 Effect on the excitation state

It is known that the excitation state of an oligomer is key to understanding the relationship between the electronic structure and the band gap of a polymer. One important tool to qualitatively judge the excitation state is associated with the HOMO–LUMO gap, Δ. The calculated HOMO–LUMO gaps as well as the HOMO and LUMO levels are illustrated in Fig. 3. The attachment of the—CH_3 group slightly destabilizes both the HOMO and LUMO levels with almost the same extent (named symmetric destabilization), as a result that the HOMO–LUMO gaps of the substituted compounds CH_3–π–CH_3 decrease only by a small value of 0.04–0.09 eV comparing to the unsubstituted ones H–π–H. The substitution of the –CN group evidently stabilizes both the HOMO and LUMO levels. Note that this stabilization is asymmetric in the sense that the LUMO level is more affected than the HOMO level. In contrast, the HOMO–LUMO gaps tend to be largely lowered by about 0.22–0.43 eV for molecules CH_3–π–CN and by 0.27–0.40 eV for molecules CN–π–CN.

Another effective technique to investigate the excitation state is by the TDDFT calculations. Convoluted profiles of the excitation spectra obtained with a Gaussian broadening for ten lowest excitation states of each compound are described in Fig. 4. Table 1 collects the TDDFT excitation

Table 1 The B3LYP/6-31G* calculated results for average tortional angle $\bar{\theta}$, average intra- and inter-ring bond alternation parameters, $\bar{\delta}_{\text{intra}}$ and $\bar{\delta}_{\text{inter}}$, and excitation energies, E_g

Compound	$\bar{\theta}$/°	$\bar{\delta}_{\text{intra}}$/Å	$\bar{\delta}_{\text{inter}}$/Å	E_g/eV (f)
X=CH_2				
1a ($R_1 = R_2 = -$H)	0.01	0.064	0.049	2.82 (0.70)
2a ($R_1 = R_2 = -CH_3$)	0.02	0.063	0.048	2.72 (0.81)
3a ($R_1 = -CH_3$, $R_2 = -$CN)	0.00	0.055	0.044	2.57 (0.90)
4a ($R_1 = R_2 = -$CN)	0.00	0.052	0.044	2.56 (1.03)
X=NH				
1b ($R_1 = R_2 = -$H)	0.06	0.023	0.039	3.93 (0.91)
2b ($R_1 = R_2 = -CH_3$)	0.02	0.023	0.039	3.82 (1.06)
3b ($R_1 = -CH_3$, $R_2 = -$CN)	0.01	0.016	0.035	3.49 (0.92)
4b ($R_1 = R_2 = -$CN)	0.02	0.011	0.034	3.55 (1.28)
X=O				
1c ($R_1 = R_2 = -$H)	0.00	0.042	0.045	3.71 (0.85)
2c ($R_1 = R_2 = -CH_3$)	0.03	0.041	0.044	3.59 (0.99)
3c ($R_1 = -CH_3$, $R_2 = -$CN)	0.00	0.035	0.041	3.31 (0.96)
4c ($R_1 = R_2 = -$CN)	0.00	0.031	0.040	3.33 (1.21)
X=SiH_2				
1d ($R_1 = R_2 = -$H)	0.00	0.071	0.049	2.58 (0.78)
2d ($R_1 = R_2 = -CH_3$)	0.01	0.069	0.048	2.52 (0.90)
3d ($R_1 = -CH_3$, $R_2 = -$CN)	0.01	0.062	0.045	2.38 (1.00)
4d ($R_1 = R_2 = -$CN)	0.01	0.059	0.044	2.34 (1.11)
X=PH				
1e ($R_1 = R_2 = -$H)	2.17	0.055	0.050	2.68 (0.68)
2e ($R_1 = R_2 = -CH_3$)	1.11	0.054	0.049	2.62 (0.80)
3e ($R_1 = -CH_3$, $R_2 = -$CN)	1.24	0.047	0.046	2.48 (0.89)
4e ($R_1 = R_2 = -$CN)	1.30	0.044	0.045	2.46 (0.99)
X=S				
1f ($R_1 = R_2 = -$H)	0.02	0.033	0.048	3.27 (0.81)
Exp.				3.50[a]/3.49[b]
2f ($R_1 = R_2 = -CH_3$)	0.00	0.031	0.047	3.18 (0.95)
Exp.				3.40[b]/3.41[c]
3f ($R_1 = -CH_3$, $R_2 = -$CN)	0.00	0.025	0.044	2.98 (0.96)
4f ($R_1 = R_2 = -$CN)	0.01	0.022	0.044	2.98 (1.14)
Exp.				3.24[a]/3.17[b]

Oscillator strengths, f, are given in the parenthesis

[a] Ref. [98]

[b] Ref. [66]

[c] Ref. [89]

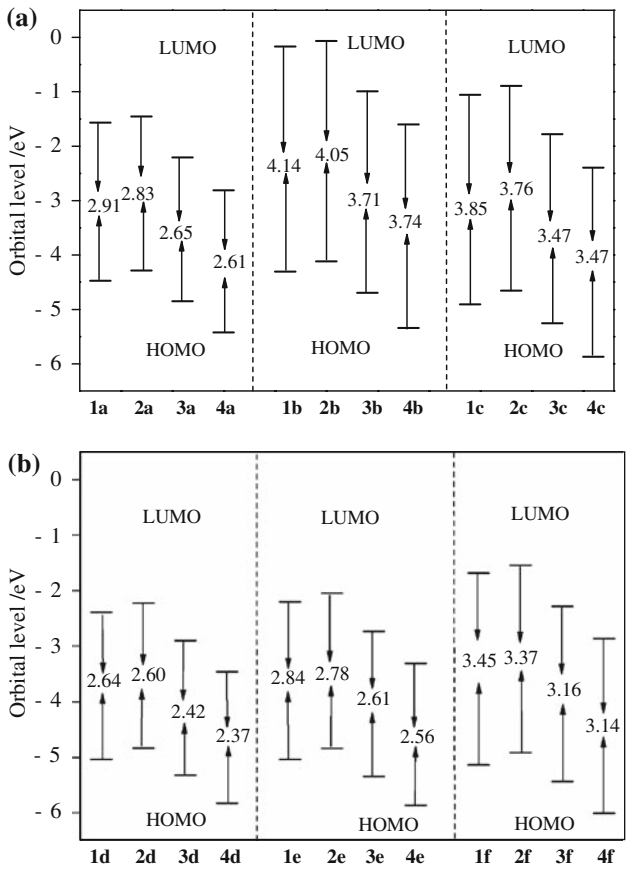

Fig. 3 The substitution effect on the HOMO and LUMO energy levels and the HOMO–LUMO gaps of (**a**) a–c and (**b**) d–f

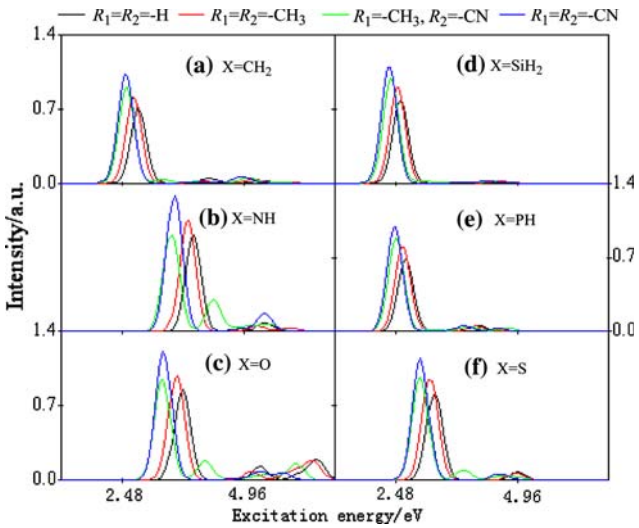

Fig. 4 The stimulated UV/Vis spectrum of the unsubstituted and substituted oligoheterocyclics

energies of the maximum absorption peaks, E_g. The spectrum of a CH_3–π–CH_3 molecule shows very similar to that of its corresponding parent compound H–π–H (only a 0.06–0.12 eV bathochromic shift of the maximum absorption peak). This negligible effect of –CH_3/–CH_3 on the UV/vis absorption spectra can be attributed to the almost symmetric destabilization of the HOMO and LUMO orbitals caused by the –CH_3/–CH_3 substitution. In contrast, the –CH_3/–CN and –CN/–CN substitutions lead to an evident bathochromic shift of about 0.20 ∼ 0.44 eV of the maximum absorption peak due to the fact that the substitution gives rise to an asymmetric stabilization of the frontier orbitals. These results are in good agreement with the experimental observations: the attachment of –CH_3/–CH_3 groups to the terthiophene ends results in a bathochromic shift of only about 0.09 eV, while the appendent of –CN/–CN groups leads to a bathochromic shift of about 0.30 eV relative to the unsubstituted terthiophene [53,66,89].

As expected, the HOMO–LUMO gaps, Δ, and the TDDFT excitation energies, E_g, show the same change tendencies. Clearly, the values of Δ and E_g of the parent molecules H–π–H decrease when the heteroatoms X going from the second row elements to the third row elements, i.e. **1a**(Δ = 2.91, E_g = 2.82 eV) > **1d** (Δ = 2.64, E_g=2.58 eV), **1b** (Δ = 4.14, E_g = 3.93 eV) > **1e** (Δ = 2.84, E_g = 2.68 eV), and **1c** (Δ = 3.85, E_g = 3.71 eV) > **1f** (Δ = 3.45, E_g = 3.27 eV) An identical trend was observed after substitutions, for examples, **2a** (Δ = 2.83, E_g = 2.72 eV) > **2d** (Δ = 2.60, E_g = 2.52 eV), **2b** (Δ = 4.05, E_g = 3.82 eV) > **2e** (Δ = 2.78, E_g = 2.62 eV), and **2c** (Δ = 3.76, E_g = 3.59 eV) > **2f** (Δ = 3.37, E_g = 3.18, eV) for CH_3–π–CH_3 molecules; **3a** (Δ = 2.65, E_g = 2.57 eV) > **3d** (Δ = 2.42, E_g = 2.38 eV), **3b** (Δ = 3.71, E_g = 3.49 eV) > **3e** (Δ = 2.61, E_g = 2.48 eV), and **3c** (Δ = 3.47, E_g = 3.31 eV) > **3f** (Δ = 3.16, E_g = 2.98 eV) for = 3.16, E_g = 2.98 eV) for CH_3–π–CN series; **4a** (Δ = 2.61, E_g = 2.56 eV) > **4d** (Δ = 2.37, **4b** (Δ = 3.74, E_g = 3.55 eV) > **4e** (Δ = 2.56, E_g = 2.46 eV), and **4c** (Δ = 3.47, E_g = 3.33 eV) > **4f** (Δ = 3.14, E_g = 2.98 eV) for CN–π–CN compounds. Therefore, the end-substitution exerts a fine-tune effect on the excitation state. Overall, the order of both Δ and E_g values for all the molecules is **b** > **c** > **f** > **a** > **e** > **d**. All the above mentioned orders can be qualitatively interpreted from the NBO analysis.

3.3 Effect on the electron conjugation

The electron conjugation effect can be reflected by the stabilization interaction energies, $E^{(2)}$, between a donor bonding orbital and an acceptor antibonding orbital obtained by the NBO analysis. If the $E^{(2)}$ value is large, strong conjugation occurs between the two bonds. The calculated stabilization energies are summarized in Table 2, where the subscript A → B of $E^{(2)}_{A\to B}$ indicates that the electrons delocalize from A to B. For examples, R → π* means that the electron transfers from the substituent R to its vicinal C=C bond; π(outer) → π*(inner) represents that an outer

Table 2 Interaction energy between electron-donating and electron-accepting orbitals, $E^{(2)}$ /kcal mol^{-1}, obtained by NBO analysis

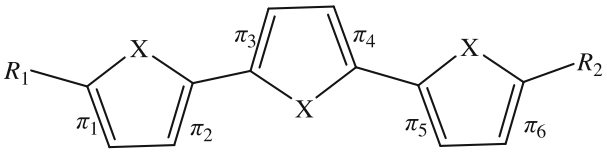

Compound	$E^{(2)}_{R_1\to\pi_1^*}$ ($E^{(2)}_{\pi_1\to R_1^*}$)	$E^{(2)}_{R_2\to\pi_6^*}$ ($E^{(2)}_{\pi_6\to R_2^*}$)	$\overline{E}^{(2)}_{\pi(\text{outer})\to\pi^*(\text{inner})}$ ($\overline{E}^{(2)}_{\pi(\text{inner})\to\pi^*(\text{outer})}$)	$\overline{E}^{(2)}_{\pi(\text{CH}_3)\to\pi^*(\text{CN})}$ ($\overline{E}^{(2)}_{\pi(\text{CN})\to\pi^*(\text{CH}_3)}$)	$\overline{E}^{(2)}_{\text{X}\to\pi^*}$ ($\overline{E}^{(2)}_{\pi\to\text{X}^*}$)
X=CH_2					
1a ($R_1 = R_2 = -$H)	0.0 (0.0)		15.9 (16.8)		11.8 (11.3)
2a ($R_1 = R_2 = -CH_3$)	7.3 (5.4)		16.4 (16.4)		11.8 (11.2)
3a ($R_1 = -CH_3$, $R_2 = -$CN)	7.4 (5.2)	9.6 (21.2)		18.4 (15.5)	11.8 (11.2)
4a ($R_1 = R_2 = -$CN)	9.8 (20.5)		15.8 (18.9)		11.8 (11.1)
X=NH					
1b ($R_1 = R_2 = -$H)	0.0 (0.0)		16.5 (17.6)		75.7 (2.8)
2b ($R_1 = R_2 = -CH_3$)	5.9 (4.0)		17.0 (16.8)		76.1 (2.8)
3b ($R_1 = -CH_3$, $R_2 = -$CN)	6.0 (3.9)	8.3 (21.8)		19.3 (16.3)	75.9 (2.8)
4b ($R_1 = R_2 = -$CN)	8.4 (21.2)		16.3 (19.7)		76.6 (2.8)
X=O					
1c ($R_1 = R_2 = -$H)	0.0 (0.0)		15.2 (16.5)		54.5 (1.7)
2c ($R_1 = R_2 = -CH_3$)	7.0 (5.2)		15.8 (15.7)		54.7 (1.6)
3c ($R_1 = -CH_3$, $R_2 = -$CN)	7.1 (5.1)	8.9 (20.6)		17.6 (14.9)	54.5 (1.7)
4c ($R_1 = R_2 = -$CN)	9.1 (20.0)		15.0 (18.3)		54.1 (1.7)
X=SiH_2					
1d ($R_1 = R_2 = -$H)	0.0 (0.0)		14.7 (15.6)		4.0 (10.6)
2d ($R_1 = R_2 = -CH_3$)	6.8 (5.3)		15.4 (15.1)		4.0 (10.5)
3d ($R_1 - CH_3$, $R_2 = -$CN)	7.0 (5.1)	9.5 (20.5)		17.0 (14.2)	4.0 (10.2)
4d ($R_1 = R_2 = -$CN)	9.8 (19.9)		14.6 (17.1)		4.1 (10.1)
X=PH					
1e ($R_1 = R_2 = -$H)	0.0 (0.0)		14.6 (15.9)		10.8 (7.7)
2e ($R_1 = R_2 = -CH_3$)	6.6 (5.2)		15.3 (15.3)		10.6 (7.3)
3e ($R_1 = -CH_3$, $R_2 = -$CN)	6.8 (5.1)	9.0 (20.5)		17.0 (14.5)	10.7 (7.1)
4e ($R_1 = R_2 = -$CN)	9.2 (18.9)		14.5 (17.4)		10.7 (7.0)
X=S					
1f ($R_1 = R_2 = -$H)	0.0 (0.0)		14.9 (15.8)		41.5 (3.3)
2f ($R_1 = R_2 = -CH_3$)	5.6 (3.9)		15.6 (15.2)		41.1 (3.3)
3f ($R_1 = -CH_3$, $R_2 = -$CN)	5.7 (3.8)	8.2 (20.6)		17.2 (14.7)	41.7 (3.3)
4f ($R_1 = R_2 = -$CN)	8.4 (20.1)		14.6 (17.2)		42.2 (3.2)

C=C bond serves as a donating bond and its vicinal inner C=C bond serves as an accepting bond; $\pi(CH_3) \to \pi^*$(CN) suggests that the electron delocalizes from C=C bond close to –CH_3 side to its vicinal C=C bond close to –CN side, that is, the electron delocalizes along the carbon backbone from $-CH_3$ side to –CN side; X $\to \pi^*$ implies that the electron transfers from the heteroatom X to the two intra-ring C=C bonds, i.e., the value of $E^{(2)}_{X\to\pi^*}$ is the total interaction energy between the heteroatom X and the two intra-ring C=C bonds.

The bonds are labeled as on the top of Table 2. The stabilization energies between π_1/π_6 orbitals and π^* orbitals of –CN are around 20.0 kcal mol^{-1} indicating a full π-electron conjugation occurs between the cyano moieties and the carbon backbone, while only a hyperconjugative effect of the methyl group contributes to the carbon backbone with the stabilization energies between σ orbitals of –CH_3 and π_1^*/π_6^* orbitals being only about 7.0 kcal mol^{-1}. As a result, the donor –CH_3/–CH_3 substitution slightly enhances the charge transfer from the outermost ring to the innermost ring, in contrast, the strong electron-withdrawing –CN/–CN substitution strengthens the charge transfer from the innermost ring toward the outermost ring. The push-pull effect of the

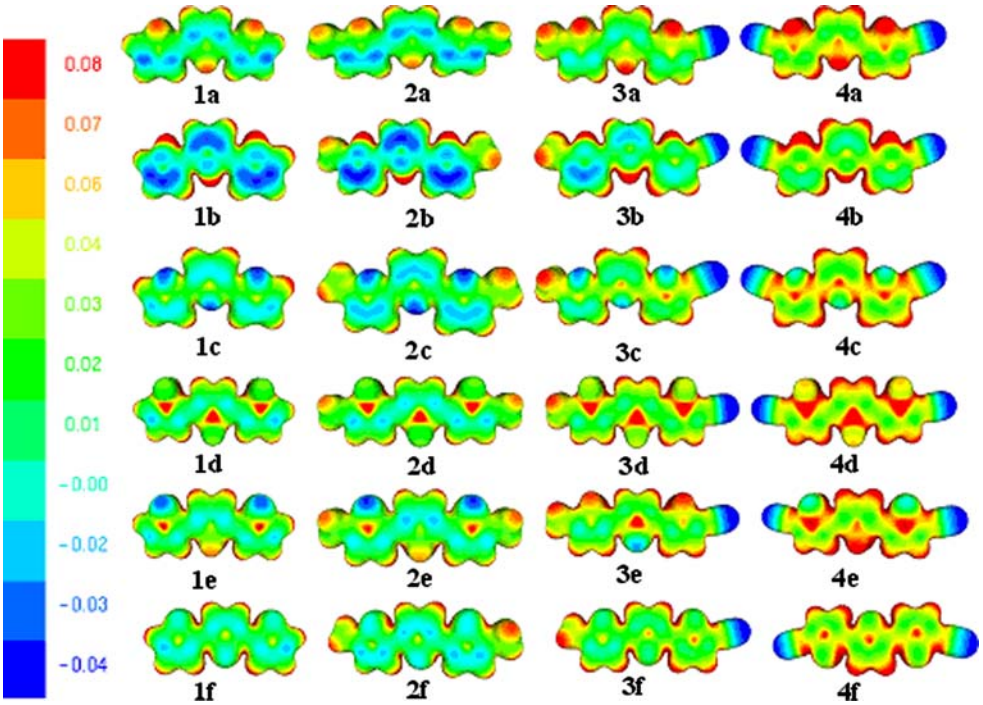

Fig. 5 The calculated B3LYP/6-31G* electrostatic potential textured vDW surfaces for the unsubstituted and substituted oligoheterocyclics

–CH_3/–CN substitution enhances the charge transfer from –CH_3 side to –CN side via the π-conjugated backbone. These cases can be confirmed from the average data of $E^{(2)}_{A\to B}$ in Table 2. Comparing to the parent H–π–H molecules ($\overline{E}^{(2)}_{\pi(\text{outer})\to\pi^*(\text{inner})}$ = 14.6–16.5 and $\overline{E}^{(2)}_{\pi(\text{inner})\to\pi^*(\text{outer})}$ = 15.6–17.6 kcal mol^{-1}), the values of $\overline{E}^{(2)}_{\pi(\text{outer})\to\pi^*(\text{inner})}$ in $CH_3-\pi-CH_3$ systems are increased by 0.4–0.7 and those of $\overline{E}^{(2)}_{\pi(\text{inner})\to\pi^*(\text{outer})}$ in CN–π–CN systems are raised by 1.4–2.1 kcal mol^{-1}. In the case of CH_3–π–CN systems, the average values of $\overline{E}^{(2)}_{\pi(CH_3)\to\pi^*(CN)}$ go up to 17.0–19.3 kcal mol^{-1}.

Strong X$\to\pi^*/\pi\to$X* interaction with large values of $\overline{E}^{(2)}_{X\to\pi^*}/\overline{E}^{(2)}_{\pi\to X^*}$ could confine more π electrons within the rings, which is unfavorable for the π electron delocalization along the chain, and consequently, the HOMO–LUMO gap and the excitation energy will be high. Table 2 also lists the average data of $\overline{E}^{(2)}_{X\to\pi^*}$ and $\overline{E}^{(2)}_{\pi\to X^*}$. There are large interactions between X and C=C* bonds for X=NH, O, and S. The data of $\overline{E}^{(2)}_{X\to\pi^*}/\overline{E}^{(2)}_{\pi\to X^*}$ for X=NH, O, and S may be overestimated as can be found using the NBO deletion procedure [90], thus, the calculated values may serve only as qualitative tools, but in this paper, the change tendency of $\overline{E}^{(2)}_{X\to\pi^*}/\overline{E}^{(2)}_{\pi\to X^*}$ is in line with the aforementioned HOMO–LUMO gaps and excitation energies: the compound with X containing the second row element has a larger $\overline{E}^{(2)}_{X\to\pi^*}/\overline{E}^{(2)}_{\pi\to X^*}$ value than that with X containing the third row element, i.e., **a** > **d**, **b** > **e**, and **c** > **f** for the unsubstituted and substituted molecules. Moreover, just as Δ and E_g, the order of $\overline{E}^{(2)}_{X\to\pi^*}/\overline{E}^{(2)}_{\pi\to X^*}$ for all the molecules is also **b** > **c** > **f** > **a** > **e** > **d**. Therefore, the X$\to\pi^*/\pi\to$X* interaction maybe a key factor to influence the HOMO–LUMO gap and the excitation energy for a planar single oligomer.

In addition, NBO analysis certainly suggests that –CH_3 and –CN substituents act as electron-donating and -accepting groups, respectively. In CH_3–π–CH_3 molecules, the total charge of the carbon backbone is negative while –CH_3 bears positive charge. The reverse is true for CN–π–CN molecules. For example, in **2f** (X=S and R_1, R_2 = $-CH_3$), $-CH_3$ has 0.008 a.u. charge while the carbon backbone has -0.008 a.u. charge; and in **4f** (X=S and R_1, R_2 = –CN), –CN has -0.182 a.u. charge while the carbon backbone has 0.182 a.u. charge. This result is in agreement with the electrostatic potential distribution as shown in the Sect. 3.4.

3.4 Effect on the p-type or n-type conductivity

The p-type or n-type conductivity of a polymer can be understood from the molecular electrostatic potential and the charge carrier (hole or electron) injection rate.

Molecular electrostatic potential. The molecular electrostatic potential is an important tool to analyze molecular reactivity because it provides information about local polarity. Figure 5 gives the distribution of the molecular electrostatic potential. There, the most negative and positive potentials are assigned

to be blue and red, respectively, and the color spectrum is mapped to all other values by linear interpolation. In the parent molecules the carbon backbones bear negative potentials. Evidently, in the substituted systems the –CH_3 moiety shows positive potential while the –CN moiety offers marked negative spatial domains. Accordingly, the negative potential of the carbon skeletons is slightly enhanced (more blue) by the –CH_3/–CH_3 substitution, while the carbon backbones switch to positive potentials after the –CN/–CN substitution. The magnitudes of potentials of the carbon skeletons for CH_3–π–CN compounds lie between CH_3–π–CH_3 and CN–π–CN analogues. Therefore, after –CH_3/–CH_3 substitutions, the carbon skeletons of **a**–**f** are expected to be easily attacked by electrophiles, i.e., to easily occur oxidizing dopings (p-type); on the contrary, after electron-accepting –CN/–CN substitutions, the carbon skeletons are supposed to be easily attacked by nucleophiles, i.e., to easily occur reducing dopings (n-type).

Charge carrier injection rate. The ionization potentials and electron affinities are closely related to the degree of the electron extraction (hole injection) to form p-type semiconductors and the electron injection to form n-type semiconductors. Although HOMO and LUMO orbital energies from density functional methods cannot be formally taken as either the ionization potential or the electron affinity, previous studies have shown that B3LYP-derived HOMO and LUMO values compare favorably with experimental ionization potentials [91] and electron affinities, respectively [91–95]. Therefore, B3LYP calculated HOMO and LUMO values can be qualitatively evaluate the ability of the charge carrier (hole or electron) injection. The simplest picture for a Schottky-type injection barrier for hoping-type carrier transport can be described by a Boltzmann-like distribution as schematically displayed in Scheme 2 [96,97]:

$$v \propto \exp\left(\frac{-\Delta E}{kT}\right) \tag{1}$$

where v is the carrier injection rate, ΔE is the magnitude of the injection barrier, $T = 298\,\mathrm{K}$, and k is the Boltzmann constant. The organic field-effect transistor and the organic light-emitting diode experiments show that Eq. (1) can satisfactorily describe the charge injection properties of electrode/organic interface. Thus, for a given electrode, the hole and electron injection rates are mainly decided by the HOMO and LUMO levels. The relationship of the charge carrier injection rate between the unsubstituted and the substituted molecules can be expressed as

$$v_e^{sub}/v_e^{unsub} = \exp\left(\frac{E_L^{unsub} - E_L^{sub}}{kT}\right) \tag{2}$$

$$v_h^{sub}/v_h^{unsub} = \exp\left(\frac{E_H^{sub} - E_H^{unsub}}{kT}\right) \tag{3}$$

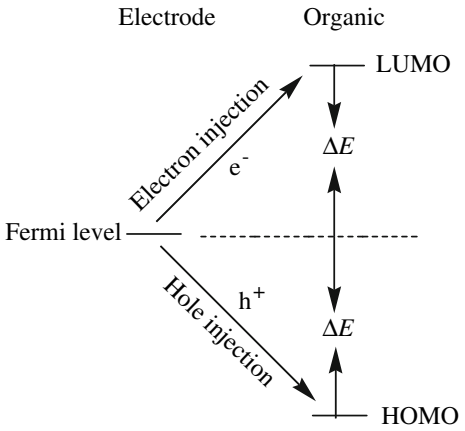

Scheme 2 Schottky-type injection barriers between an electrode and an organic semiconductor

where v_e^{sub} and v_e^{unsub} are the electron injection rates for the substituted and unsubstituted molecules, respectively; E_L^{sub} and E_L^{unsub} are the LUMO energies for the substituted and unsubstituted molecules, respectively; v_h^{sub} and v_h^{unsub} are the hole injection rates for the substituted and unsubstituted molecules, respectively; E_H^{sub} and E_H^{unsub} are the HOMO energies for the substituted and unsubstituted molecules, respectively. Here, we assume that the HOMO and LUMO levels of the unsubstituted molecules are zero, accordingly, their carrier injection rates equal to 1.00. Table 3 lists the relative HOMO/LUMO levels and the carrier injection rates for each family relative to the unsubstituted molecules. Due to the exponential dependence of carrier inject rate on ΔE, difference of a few barrier height can significantly influence the injection rate. The hole injection rates are increased by ca. 10^2–10^4 times for the –CH_3/–CH_3 substitution, while the electron injection rates are increased by ca. 10^8–10^{13} and 10^{17}–10^{24} times for –CH_3/–CN and –CN/–CN substitutions, respectively. Therefore, –CH_3/–CH_3 substitution enhances the p-type characteristic by increasing the HOMO levels, while –CH_3/–CN and –CN/–CN substitutions strengthen the n-type conductivity by decreasing the LUMO levels.

In practice, the substitution technique is usually used to tune the doping types for designing novel materials with desirable conductive behavior. For example, the unsubstituted and the –CH_3/–CH_3 end-capped oligothiophenes show p-type conductivity [20,89,98–101], while the –CN/–CN end-capped oligothiophenes exhibit n-type transport [11,66,102,103].

3.5 Effect on charge carrier hoping channels between chains

The atoms in molecules methodology (AIM) has been successfully applied in qualitatively elucidating the inter-chain charge carrier hoping channels of solid furan by using Bader's topological analysis of the charge electron density, ρ [104].

Table 3 The relative HOMO/LUMO levels, electron injection rates, v_e, and hole injection rates, v_h to unsubstituted oligomers

Compound	Relative HOMO energy/eV	Relative LUMO energy/eV	v_e	v_h
X=CH_2				
1a ($R_1 = R_2 = -H$)	0.000	0.000	1.00	1.00
2a ($R_1 = R_2 = -CH_3$)	0.187	0.113	1.23E-02	1.45E+02
3a ($R_1 = -CH_3$, $R_2 = -CN$)	−0.375	−0.638	6.16E+10	4.55E−07
4a ($R_1 = R_2 = -CN$)	−0.948	−1.244	1.09E+21	9.28E-17
X=NH				
1b ($R_1 = R_2 = -H$)	0.000	0.000	1.00	1.00
2b ($R_1 = R_2 = -CH_3$)	0.191	0.104	1.74E-02	1.70E+03
3b ($R_1 = -CH_3$, $R_2 = -CN$)	−0.389	−0.822	7.97E+13	2.64E-07
4b ($R_1 = R_2 = -CN$)	−1.036	−1.433	1.72E+24	3.01E-18
X=O				
1c ($R_1 = R_2 = -H$)	0.000	0.000	1.00	1.00
2c ($R_1 = R_2 = -CH_3$)	0.251	0.163	1.75E-03	1.76E+04
3c ($R_1 = -CH_3$, $R_2 = -CN$)	−0.350	−0.726	1.90E+12	1.20E-06
4c ($R_1 = R_2 = -CN$)	−0.964	−1.340	4.59E+22	4.98E-17
X=SiH_2				
1d ($R_1 = R_2 = -H$)	0.000	0.000	1.00	1.00
2d ($R_1 = R_2 = -CH_3$)	0.205	0.165	1.62E-03	2.93E+03
3d ($R_1 = -CH_3$, $R_2 = -CN$)	−0.290	−0.508	3.90E+08	1.25E-05
4d ($R_1 = R_2 = -CN$)	−0.789	−1.062	9.13E+17	4.53E-14
X=PH				
1e ($R_1 = R_2 = -H$)	0.000	0.000	1.00	1.00
2e ($R_1 = R_2 = -CH_3$)	0.203	0.151	2.79E-03	2.71E+03
3e ($R_1 = -CH_3$, $R_2 = -CN$)	−0.309	−0.537	1.21E+09	5.94E-06
4e ($R_1 = R_2 = -CN$)	−0.828	−1.101	4.17E+18	9.93E-15
X=S				
1f ($R_1 = R_2 = -H$)	0.000	0.000	1.00	1.00
2f ($R_1 = R_2 = -CH_3$)	0.224	0.144	3.67E-03	6.14E+03
3f ($R_1 = -CH_3$, $R_2 = -CN$)	−0.300	−0.594	1.11E+10	8.44E-06
4f ($R_1 = R_2 = -CN$)	−0.870	−1.177	8.04E+19	1.93E-15

The localizations of the critical points (CPs) in the ρ and the values of its Laplacian, $\nabla^2\rho$, at these points have shown to be very suitable tools for the characterization of molecular electronic structure in terms of the nature and magnitude of the interactions. The CPs are the points at which the gradient of the scalar field vanishes. The CPs are further characterized from the eigenvalues of the Hessian matrix of ρ, which have two negative and one positive eigenvalues correspond to bond critical point (BCP) (3, −1). The sign of the Laplacian, $\nabla^2\rho$, at (BCP) (3, −1) indicates that the charge electron density is either locally depleted ($\nabla^2\rho > 0$) such as ion bonds, hydrogen bonds, and van der Waals bonds or locally concentrated ($\nabla^2\rho < 0$) such as covalent and polar bonds.

It is known that the inter-chain charge carrier transfer is of fundamental importance in understanding the conductivity of oligomers. The presence of the substituents R would introduce additional intermolecular interactions such as $R\cdots\pi$, $R\cdots R$, $R\cdots H$, and $R\cdots X$ interactions, which may play an important role in charge carrier hopings between neighboring chains. Some of these interactions have already been experimentally detected in the –CH_3/–CH_3 and –CN/–CN substituted oligothiophene crystals [65,66,103]. The packing dimer formed by two substituted monomers as displayed in Fig. 2 is a prototype model to investigate the intermolecular bond paths induced by the substituents R. Various packing orientations of two monomers may occur in a real packing system. In this paper, some special orientation pairs as given in Fig. 2 are selected to carry out the AIM calculations. The atoms in the substituent R of one ring used to interact with another ring are numbered as 1 and 2, and the carbon atoms of another ring are labeled as 3, 4, 5, and 6 (cf. $\mathbf{a}_1$, $\mathbf{b}_1$ and $\mathbf{c}_1$ in Figs. 2 and 6, S1, and S2). In models $\mathbf{a}_1$, $\mathbf{b}_1$ and $\mathbf{c}_1$, the line C_3C_5 intersects the line C_4C_6 at M. C_1–H_2 bond in models $\mathbf{a}_1$ and $\mathbf{b}_1$ and $C_1{\equiv}N_2$ bond in model $\mathbf{c}_1$ point directly to M. In models $\mathbf{a}_{2-7}$, $\mathbf{b}_{2-7}$ and $\mathbf{c}_{2-7}$, atoms of the intermolecular contact bonds are in a line. The C_1–H_2 bonds in models $\mathbf{a}_{8-11}$ and $\mathbf{b}_{8-11}$ and the $C_1{\equiv}N_2$ bonds in models $\mathbf{c}_{8-11}$ directly point to the heteroatoms X (N, P, O, and S) and perpendicular to the ring plane of another monomer. Here we assume that the contacts (represented by the dot lines in Fig. 2) of the packing pairs for studying intermolecular interactions are separated by 3.5 Å.

Figure 6 shows the bond paths for –CN/–CN substituted packing dimers, for the sake of conciseness, those for unsubstituted and –CH_3/–CH_3 substituted packing dimers are available in Figs. S1 and S2 as Supporting Information. The electronic density ρ and its Laplacian $\nabla^2\rho$ of the BCPs are listed in Tables 4–6, from which it can be seen that for a given interaction type, the intermolecular interactions have similar values of ρ and $\nabla^2\rho$ regardless of what kinds of heteroatoms. For example, for the $H\cdots H$ interactions, the ρ and $\nabla^2\rho$ are all around 0.003–0.004 and 0.010–0.012 a.u., respectively.

$R\cdots\pi$ interaction. First, we consider the $R\cdots\pi$ contacts of $\mathbf{a}_1$, $\mathbf{b}_1$, and $\mathbf{c}_1$ in Figs. 2 and 6, S1, and S2. Figures 6, S1, and S2 clearly demonstrate the existence of the bond paths and their corresponding BCPs for $H_2\cdots C_3$ and $H_2\cdots C_6$ contacts in the parent packing dimer $\mathbf{a}_1$ and the CH_3-substituted packing dimer $\mathbf{b}_1$, and for $N_2\cdots C_3$ and $N_2\cdots C_6$ contacts in the CN-substituted packing dimer $\mathbf{c}_1$. The contacts $C_1-H_2\cdots C_3$ and C_1–$H_2\cdots C_6$ in $\mathbf{a}_1$ and $\mathbf{b}_1$ should be classified as the C–H$\cdots\pi$ interactions. The $C_1{\equiv}N_2\cdots C_3$ and $C_1{\equiv}N_2\cdots C_6$ contacts in $\mathbf{c}_1$ should be regarded as C≡N$\cdots\pi$ interactions.

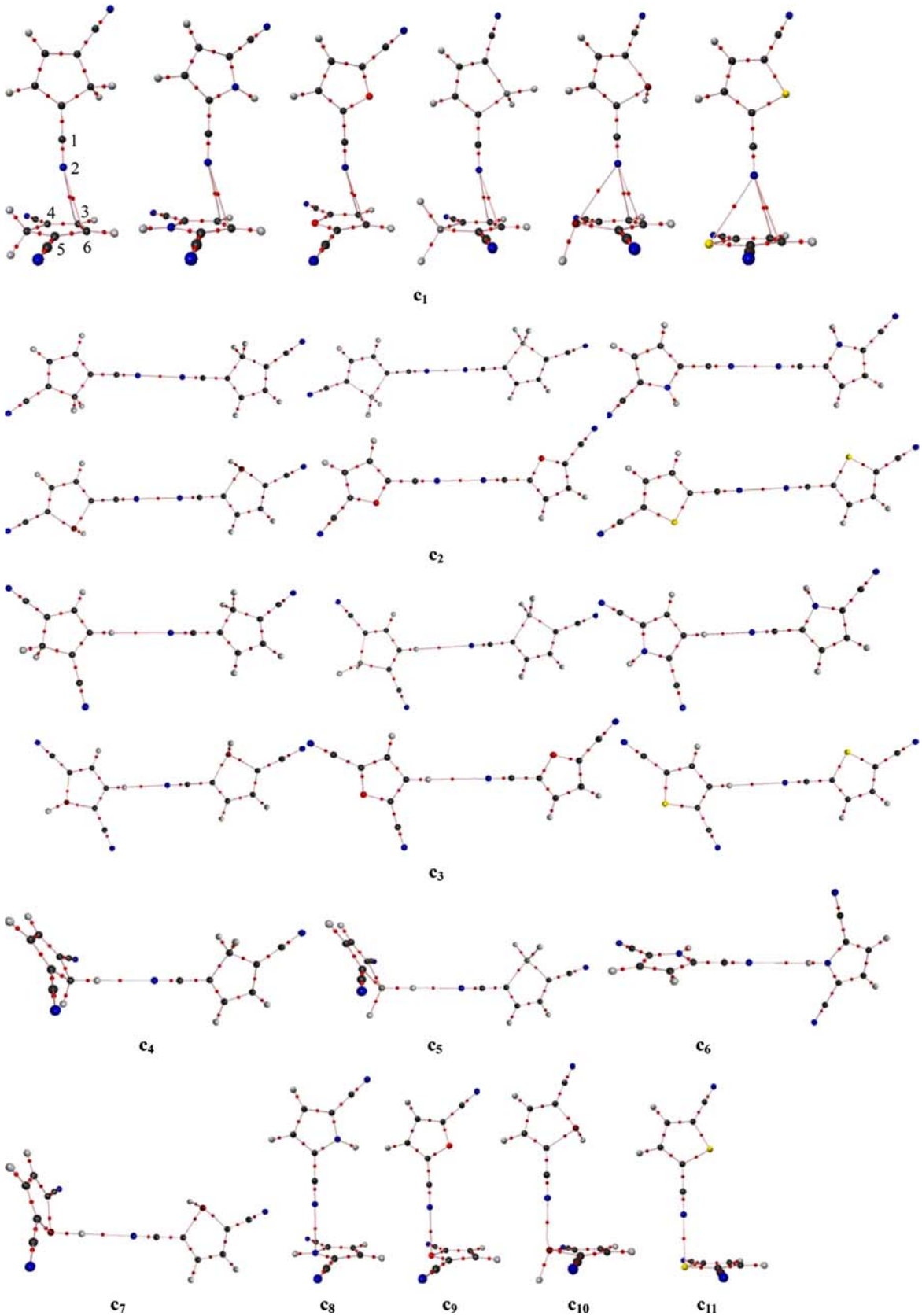

Fig. 6 The location of the BCP (*red dot*) of intermolecular contacts in the CN-substituted packing dimers. $\mathbf{c}_1$ for R $\cdots$ π interaction, $\mathbf{c}_2$ for R $\cdots$ R interaction, $\mathbf{c}_{3-7}$ for R $\cdots$ H interaction, and $\mathbf{c}_{8-11}$ for R $\cdots$ X interaction

Table 4 The electron density (ρ) and the Laplacian of the electron density ($\nabla^2\rho$) of the BCP for the contact bonds of the unsubstituted packing dimers **a** (in unit a.u.)

Interaction	Dimer	ρ	$\nabla^2\rho$
R···π (C–H···π)	$\mathbf{a}_1$		
	X=CH_2	0.008	0.028
	X=NH	0.009	0.029
	X=O	0.008	0.029
	X=SiH_2	0.008	0.028
	X=PH	0.008	0.028
	X=S	0.008	0.029
R···R (H···H)	$\mathbf{a}_2$		
	X=CH_2	0.003	0.011
	X=NH	0.003	0.011
	X=O	0.003	0.011
	X=SiH_2	0.003	0.011
	X=PH	0.003	0.011
	X=S	0.003	0.011
R··· H (H···H)	$\mathbf{a}_3$		
	X=CH_2	0.003	0.011
	X=NH	0.003	0.011
	X=O	0.003	0.011
	X=SiH_2	0.003	0.011
	X=PH	0.003	0.011
	X=S	0.003	0.011
	$\mathbf{a}_4$	0.003	0.011
	$\mathbf{a}_5$	0.004	0.012
	$\mathbf{a}_6$	0.003	0.010
	$\mathbf{a}_7$	0.004	0.011
R··· X (C–H···N)	$\mathbf{a}_8$	0.010	0.032
(C–H···P)	$\mathbf{a}_9$	0.016	0.042
(C–H···O)	$\mathbf{a}_{10}$	0.009	0.031
(C–H···S)	$\mathbf{a}_{11}$	0.016	0.047

Table 5 The electron density (ρ) and the Laplacian of the electron density ($\nabla^2\rho$) of the BCP for the contact bonds of the CH_3-substituted packing dimers **b** (in unit a.u.)

Interaction	Dimer	ρ	$\nabla^2\rho$
R···π (C–H···π)	$\mathbf{b}_1$		
	X=CH_2	0.009	0.029
	X=NH	0.009	0.030
	X=O	0.009	0.030
	X=SiH_2	0.008	0.028
	X=PH	0.008	0.028
	X=S	0.008	0.029
R···R (H···H)	$\mathbf{b}_2$		
	X=CH_2	0.003	0.011
	X=NH	0.003	0.011
	X=O	0.003	0.011
	X=SiH_2	0.004	0.012
	X=PH	0.003	0.011
	X=S	0.003	0.011
R··· H (H···H)	$\mathbf{b}_3$		
	X=CH_2	0.003	0.011
	X=NH	0.003	0.011
	X=O	0.003	0.011
	X=SiH_2	0.004	0.011
	X=PH	0.003	0.011
	X=S	0.003	0.011
	$\mathbf{b}_4$	0.004	0.011
	$\mathbf{b}_5$	0.004	0.011
	$\mathbf{b}_6$	0.003	0.010
	$\mathbf{b}_7$	0.004	0.012
R··· X (C–H···N)	$\mathbf{b}_8$	0.011	0.033
(C–H···P)	$\mathbf{b}_9$	0.017	0.043
(C–H···O)	$\mathbf{b}_{10}$	0.009	0.032
(C–H···S)	$\mathbf{b}_{11}$	0.016	0.049

It is clear from Tables 4–6 that all the Laplacians for R···π interactions take positive values suggesting the typical closed interactions. The values of ρ (0.008–0.009 a.u.) or $\nabla^2\rho$(0.028–0.030 a.u.) for the C–H···π interactions are found to be close between the parent packing dimers $\mathbf{a}_1$ and the CH_3-substituted packing dimers $\mathbf{b}_1$. Therefore, the strengths of C–H···π interactions in the CH_3-substituted $\mathbf{b}_1$ are very similar to those in the unsubstituted $\mathbf{a}_1$. In contrast, the values of ρ and $\nabla^2\rho$ for C≡N···π interactions in $\mathbf{c}_1$(ρ : 0.018–0.019 a.u.; $\nabla^2\rho$: 0.073–0.078 a.u.) are much higher than those for C–H···π interactions indicating that the –CN groups exerts stronger C≡N···π interactions than the –H and –CH_3 groups do for C–H···π interactions.

R···R interaction. Second, we treat with the R···*R* interactions as illustrated in $\mathbf{a}_2$,$\mathbf{b}_2$, and $\mathbf{c}_2$ in Figs. 2, 6, S1, and S2. In the unsubstituted $\mathbf{a}_2$ and the CH_3-substituted $\mathbf{b}_2$, the R···R interaction is actually the H···H interaction, which was found where a bond path exist in Figs. S1 and S2 with the similar values for the density and Laplacian being about 0.003–0.004 and 0.011–0.012 a.u., respectively. While in the CN-substituted $\mathbf{c}_2$, the R···R interaction is in fact the N···N interactions, which was linked by a bond path in Fig. 6 with values about 0.024 a.u. for ρ and about 0.096–0.103 a.u. for $\nabla^2\rho$, higher than those for H···H and C–H···π interactions.

R···H interaction. In the unsubstituted packing dimers $\mathbf{a}_{3-7}$ and the CH_3-substituted packing dimers $\mathbf{b}_{3-7}$, the R···H interactions are still H···H interactions (cf. Figs. 6, S1, and S2) with similar strength to the R···R interaction (ρ: ca. 0.003–0.004 a.u.,$\nabla^2\rho$: ca. 0.010–0.012 a.u.). As can be seen in Fig. 6, the R···H interaction in the CN-substituted packing dimers $\mathbf{c}_{3-7}$ revealed a C≡N···H bond path with values for the ρ and $\nabla^2\rho$ being in the range of 0.008–0.010 and

Table 6 The electron density (ρ) and the Laplacian of the electron density ($\nabla^2\rho$) of the BCP for the contact bonds of the CN-substituted packing dimers **c** (in unit a.u.)

Interaction	Dimer	ρ	$\nabla^2\rho$
R···π (C≡N···π)	$\mathbf{c}_1$		
	X=CH_2	0.018	0.074
	X=NH	0.019	0.078
	X=O	0.019	0.077
	X=SiH_2	0.018	0.073
	X=PH	0.019	0.076
	X=S	0.019	0.076
R···R (N··· N)	$\mathbf{c}_2$		
	X=CH_2	0.024	0.103
	X=NH	0.024	0.096
	X=O	0.024	0.103
	X=SiH_2	0.024	0.103
	X=PH	0.024	0.103
	X=S	0.024	0.103
R··· H (C≡N··· H)	$\mathbf{c}_3$		
	X=CH_2	0.009	0.030
	X=NH	0.009	0.030
	X=O	0.009	0.030
	X=SiH_2	0.010	0.030
	X=PH	0.010	0.030
	X=S	0.009	0.030
	$\mathbf{c}_4$	0.010	0.030
	$\mathbf{c}_5$	0.010	0.032
	$\mathbf{c}_6$	0.008	0.028
	$\mathbf{c}_7$	0.010	0.031
R··· X (C≡N··· N)	$\mathbf{c}_8$	0.025	0.108
(C≡N··· P)	$\mathbf{c}_9$	0.036	0.105
(C≡N··· O)	$\mathbf{c}_{10}$	0.023	0.099
(C≡N··· S)	$\mathbf{c}_{11}$	0.037	0.136

0.028–0.032 a.u., respectively. The C≡N···H bond is well known to be a typical hydrogen bond, whose existence have already been demonstrated by experiment [65,66]. This kind of C≡N···H interaction is stronger than H···H interaction but weaker than N···N and C≡N···π interactions and close to C–H···π interaction.

R···X interaction. In the parent packing dimers, the C–H···X (X=N, O, P, S) bond paths were found in models $\mathbf{a}_{8-11}$: $\rho = 0.010$ a.u. and $\nabla^2\rho = 0.032$ a.u. for C–H···N interaction, $\rho = 0.016$ a.u. and $\nabla^2\rho = 0.042$ a.u. for C–H···P interaction, $\rho = 0.009$ a.u. and $\nabla^2\rho = 0.031$ a.u. for C–H···O interaction, and $\rho = 0.016$ a.u. and $\nabla^2\rho = 0.047$ a.u. for C–H···S interaction, respectively. It seems that the C–H···X interaction is stronger when X is the third row element than that when X is the second row element. When –CH_3 is bounded to the ring, the R···X in $\mathbf{b}_{8-11}$ still exhibits C–H···X interaction with similar strength to those for the unsubstituted packing dimers $\mathbf{a}_{8-11}$. It is worth notice, when –CN is attached to the ring, the R···X interaction in $\mathbf{c}_{8-11}$ becomes the C≡N···X (X=N, O, P, S) interaction with larger ρ and $\nabla^2\rho$values comparing to the corresponding C–H···X interaction: $\rho = 0.025$ a.u. and $\nabla^2\rho = 0.108$ a.u. for C≡N···N interaction, $\rho = 0.036$ a.u. and $\nabla^2\rho = 0.105$ a.u. for C≡N···P interaction, $\rho = 0.023$ a.u. and $\nabla^2\rho = 0.099$ a.u. for C≡N···O interaction, and $\rho = 0.037$ a.u. and $\nabla^2\rho = 0.136$ a.u. for C≡N···S interaction. It is also found that the C≡N···X interaction is stronger when X is the third row element than that when X is the second row element.

In summery, the CH_3-substituted packing dimers exert similar intermolecular interactions (C–H···π, H···H and C–H···X) to the unsubstituted ones. Noticeably, CN-substituted packing dimers yield much stronger intermolecular interactions (C≡N···π, C≡N···H, N···N, and C≡N···X) comparing to the CH_3-substituted ones. This special function of –CN group may root in the rich-electron behavior of the N atom. Importantly, a given type interaction shows the similar interaction strength regardless what kind of derivatives. It is likely that similar intermolecular interactions exist in their corresponding polymers either between end groups or between end group and other points on the conjugated system, which could contribute to the final conducting properties in conjugated polymers. It could be anticipated that the –CN substitution is beneficial to the charge carrier hopings between chains and thereby enhance the conductivity. For example, the conductivity of 10^{-6} S/cm [100] of the unsubstituted sexithiophene is increased to 4×10^{-6} S/cm [11] after –CN/–CN attachment to the end-positions.

4 Conclusion

The end-substitution effects on the geometry, the excitation states, the electron conjugation, the conducting type (p- or n-type), and the inter-chain charge carrier hoping channels of oligoheterocycles are systematically studied using the density functional theory. It is found that the influence of the end-substitution does not depend on the heteroatom. End-substitutions play fine-tune effects on geometries and excitation states, which can be interpreted by the conjugation effects from NBO analysis. The influences on the conducting type and the inter-chain charge carrier hoping channels are much different between electron-donating –CH_3/–CH_3 and -accepting –CN/–CN substitutions. Both molecular electrostatic potentials and charge carrier injection rates indicate that the –CH_3/–CH_3 substitution is beneficial to the p-type doping, while the –CN/–CN substitution is in favor of the n-type doping. In practice, the substitution technique is usually used to switch the doping types for designing novel materials with

desirable conductive properties. The CH_3-substituted packing dimers exert similar intermolecular interactions to the unsubstituted ones. The CN-substituted packing dimers yield much stronger intermolecular interactions comparing to the $–CH_3$ substituted ones. It is likely that similar intermolecular interactions exist in their corresponding polymers. It could be anticipated that the –CN substitution is helpful to the charge carrier hopings between chains and thereby enhance the conductivity.

Acknowledgments The authors thank the reviewers for their constructive and pertinent comments. The authors thank the NSF of China (50743013, 20272011), the NSF of Heilongjiang province of China (TA2005-15, B200605), the SF for Key Teachers of University of Heilongjiang province of China (1151G019, 1152G010), the SF for leading experts in academe of Harbin City of China (2007RFXXG027), the SF for Postdoctoral of Heilongjiang province of China (LBH-Q07058), and the SF for elitists of Harbin University of Science and Technology, for the financial supports.

References

1. Meng H, Zheng J, Lovinger AJ, Wang BC, Van Patten PG, Bao Z (2003) Chem Mater 15:1778
2. Mushrush M, Facchetti A, Lefenfeld M, Katz HE, Marks TJ (2003) J Am Chem Soc 125:9414
3. Knupfer M, Liu X (2006) Surface Science 600:3978
4. Casado J, Hernández V, Delgado MCR, Ortiz RP, Navarrete JTL, Facchetti A, Marks T (2005) J Am Chem Soc 127:13364
5. Li L, Collard DM (2005) Macromolecules 38:372
6. Facchetti A, Yoon MH, Sterm CL, Hutchison GR, Ratner MA, Marks TJ (2004) J Am Chem Soc 126:13480
7. Facchetti A, Mushrush M, Yoon MH, Hutchison GR, Ratner MA, Marks TJ (2004) J Am Chem Soc 126:13859
8. Facchetti A, Mushrush M, Katz HE, Marks TJ (2003) Adv Mater 15:33
9. Facchetti A, Yoon MH, Sterm CL, Katz HE, Marks TJ (2003) Angew Chem Int Ed 42:3900
10. Facchetti A, Yoon MH, Katz HE, Mushrush M, Marks TJ (2003) Mater Res Soc Symp Proc 771:397
11. Yassar A, Demanze F, Jaafari A, Idrissi ME, Coupry C (2002) Adv Funct Mater 12:699
12. Facchetti A, Deng Y, Wang A, Koide Y, Sirringhaus H, Marks TJ, Friend RH (2000) Angew Chem Int Ed 39:4547
13. Zhang C, Sun SJ (2007) Polym Sci Part A Polym Chem 45:41
14. Yoon MH, DiBenedetto SA, Facchetti A, Marks TJ (2005) J Am Chem Soc 127:1348
15. Casado J, Zgierski MZ, Hicks RG, Myles DJT, Viruela PM, Ortí E, Delgado MCR, Hernández V, Navarrete JTL (2005) J Phys Chem A 109:11275
16. Newman CR, Frisbie CD, da Silva Filho DA, Brédas JL, Ewbank PC, Mann KR (2004) Chem Mater 16:4436
17. Casado J, Miller LL, Mann KR, Pappenfus TM, Higuchi H, Ortå E, Milián B, Pou-Amérigo R, Hernández V, Navarrete JTL (2002) J Am Chem Soc 124:12380
18. Katz HE, Dodabalapur A, Torsi L, Elder D (1995) Chem Mater 7:2238
19. Bauerle P, Segelbacherf U, Maier A, Mehring M (1993) J Am Chem Soc 115:10217
20. Hotta S, Waragai K (1991) J Mater Chem 1:835
21. Waragai K, Hotta S (1991) Synth Met 41:519
22. Garnier F, Yassar A, Hajlaoui R, Horowitz G, Deloffre D, Servet B, Ries S, Alnot P (1993) J Am Chem Soc 115:8716
23. Cai X, Burand MW, Newman CR, daSilva Filho DA, Pappenfus TM, Bader MM, Brédas JL, Mann KR, Frisbie CD (2006) J Phys Chem B 110:14590
24. Facchetti A, Letizia J, Yoon MH, Mushrush M, Katz HE, Marks TJ (2004) Chem Mater 16:4715
25. Barbarella G, Pudova O, Arbizzani C, Mastragostino M, Bongini A (1998) J Org Chem 63:1742
26. Donat-Bouillud A, Mazerolle L, Gagnon P, Goldenberg L, Petty MC, Leclerc M (1997) Chem Mater 9:2815
27. Amao K, Uchida M, Izumizawa T, Furukawa K, Yamaguchi S (1996) J Am Chem Soc 118:11974
28. Ho HA, Brisset H, Elandaloussi E, Frère P, Roncali J (1996) Adv Mater 8:990
29. Hissler M, Dyer PW, Réau R (2003) Coord Chem Rev 244:1
30. Ma J, Li S, Jiang Y (2002) Macromolecules 35:1109
31. Salznar U, Lagowski JB, Pickup PG, Poirier RA (1998) Synth Met 96:177
32. Lee SH, Jang BB, Kafafi ZH (2005) J Am Chem Soc 127:9071
33. Wang F, Luo J, Yang K, Chen J, Huang F, Cao Y (2005) Macromolecules 38:2253
34. Boydstom AJ, Yin Y, Pagenkopf BL (2004) J Am Chem Soc 126:10350
35. Chen J, Peng H, Law CCW, Dong Y, Law JWY, Williams ID, Tang BZ (2003) Macromolecules 36:4319
36. Chen J, Xie Z, Law JWY, Law CCW, Tang BZ (2003) Macromolecules 36:1108
37. Liu Y, Stringfellow TC, Ballweg D, Guzei LA, West R (2002) J Am Chem Soc 124:49
38. Yamaguchi S, Jin R, Tamao K (1999) J Am Chem Soc 121:2937
39. Yamaguchi S, Jin R, Itami Y, Goto T, Tamao K (1999) J Am Chem Soc 121:10420
40. Yamaguchi S, Jin R, Tamao K, Sato F (1998) J Org Chem 63:10060
41. Hissler M, Lescop C, Réau RCR (2005) Chimie 8:1186
42. Hissler M, Lescop C, Réau R (2005) J Organomet Chem 690:2482
43. Fave C, Hissler M, Kárpáti T, Rault-Berthelot J, Deborde V, Toupet L, Nyulászi L, Réau R (2004) J Am Chem Soc 126:6058
44. Morisaki Y, Aiki Y, Chujo Y (2003) Macromolecules 36:2594
45. Hay C, Hissler M, Fischmeister C, Rault-Berthelot J, Toupet L, Nyulászi L, Réau R (2001) Chem Eur J 7:4222
46. Deschamps E, Ricard L, Mathey F (1994) Angew Chem Int Ed Engl 33:1158
47. Hutchison GR, Ratner MA, Marks TJ (2005) J Phys Chem B 109:3126
48. Casado J, Hernández V, Delgado MCR, Ortiz RP, Navarrete JTL, Facchetti A, Marks T (2005) J Am Chem Soc 127:13364
49. Casanovas J, Zanuy D, Alemán C (2005) Polymer 46:9452
50. Salzner U (2001) Synth Met 119:215
51. De Oliveira MA, Duarte HA, Pernaut JM, De Almeida WB (2000) J Phys Chem A 104:8256
52. Salzner U (1999) Synth Met 101:482
53. Demanze F, Cornil J, Garnier F, Horowitz G, Valat P, Yassar A, Lazzaroni R, Brédas JL (1997) J Phys Chem B 101:4553
54. Distefano G, Colle MD, Jones D, Zambianchi M, Favaretto L, Modelli A (1993) J Phys Chem 97:3504
55. Zhang G, Pei Y, Ma J, Yin K, Chen C (2004) J Phys Chem B 108:6988
56. Curtis MD, Cao J, Kampf JW (2004) J Am Chem Soc 126:4318
57. Bader MM, Custelcean R, Ward MD (2003) Chem Mater 15:616
58. Pappenfus TM, Chesterfield RJ, Frisbie CD, Mann KR, Casado J, Raff JD, Miller LL (2002) J Am Chem Soc 124:4184
59. Cornil J, Calbert JP, Beljonne D, Silbey R, Brédas JL (2001) Synth Met 119:1
60. Beljonne D, Cornil J, Silbey R, Millié P, Brédas JL (2000) J Chem Phys 112:4749

61. Cornil J, Beljonne D, Dos Santos DA, Calbert JP, Shuai Z, Brédas JL (2000) Org Electrolum 4:403
62. Brédas JL, Cornil J, Beljonne D, Dos Santos DA, Shuai Z (1999) Acc Chem Res 32:267
63. Barbarella G, Zambianchi M, Antolini L, Ostoja P, Maccagnani P, Bongini A, Marseglia EA, Tedesco E, Gigli G, Cingolani R (1999) J Am Chem Soc 121:8920
64. Siegrist T, Fleming RM, Haddon RC, Laudise RA, Lovinger AJ, Katz HE, Bridenbaugh P, Davis DD (1995) J Mater Res 10:2170
65. Marseglia EA, Grepioni F, Tedesco E, Braga D (2000) Mol Cryst Liq Cryst 348:137
66. Barclay TM, Cordes AW, MacKinnon CD, Oakley RT, Reed RW (1997) Chem Mater 9:981
67. Parr RG, Yang W (1989) Density-functional theory of atoms and molecules. Oxford University Press, New York
68. Frisch MJ, Trucks GW, Schlegel HB, Scuseria GE, Robb MA, Cheeseman JR, Montgomery JA Jr, Vreven T, Kudin KN, Burant JC, Millam JM, Iyengar SS, Tomasi J, Barone V, Mennucci B, Cossi M, Scalmani G, Rega N, Petersson GA, Nakatsuji H, Hada M, Ehara M, Toyota K, Fukuda R, Hasegawa J, Ishida M, Nakajima T, Honda Y, Kitao O, Nakai H, Klene M, Li X, Knox JE, Hratchian HP, Cross JB, Adamo C, Jaramillo J, Gomperts R, Stratmann RE, Yazyev O, Austin AJ, Cammi R, Pomelli C, Ochterski JW, Ayala PY, Morokuma K, Voth GA, Salvador P, Dannenberg JJ, Zakrzewski VG, Dapprich S, Daniels AD, Strain MC, Farkas O, Malick DK, Rabuck AD, Raghavachari K, Foresman JB, Ortiz JV, Cui Q, Baboul AG, Clifford S, Cioslowski J, Stefanov BB, Liu G, Liashenko A, Piskorz P, Komaromi I, Martin RL, Fox DJ, Keith T, Al-Laham MA, Peng CY, Nanayakkara A, Challacombe M, Gill PMW, Johnson B, Chen W, Wong MW, Gonzalez C, Pople JA (2003) Gaussian 03. Gaussian, Inc., Pittsburgh
69. Becke AD (1993) J Chem Phys 98:1372
70. Zhang G, Ma J, Jiang Y (2005) J Phys Chem B 109:13499
71. Cao H, Ma J, Zhang G, Jiang Y (2005) Macromolecules 38:1123
72. Zhang G, Ma J, Jiang Y (2003) Macromolecules 36:2130
73. Levine ZH, Soven P (1984) Phys Rev A 29:625
74. Zangwill A, Soven P (1980) Phys Rev A 21:1561
75. Carpenter JE, Weinhold F (1988) J Mol Struct (Theochem) 169: 41
76. Reed AE, Curtiss LA, Weinhold F (1988) Chem Rev 88:899
77. Reed AE, Weinstock RB, Weinhold F (1985) J Chem Phys 83:735
78. Foster JP, Weinhold F (1980) J Am Chem Soc 102:7211
79. Boris B, Petia B (1999) J Phys Chem A 103:6793
80. Gadre SR, Bhadane PK (1999) J Phys Chem A 103:3512
81. Politzer P, Nurray JS (1996) In molecular electrostatic potentials: concepts and applications. In: Murray JS, Sen KD (eds) Elsevier, Amsterdam, p 649
82. Bergman DL, Laaksonen L, Laaksonen A (1997) J Mol Graph Model 15:301
83. Laaksonen L (1992) J Mol Graph 10:33
84. Bader RFW (1990) Atoms in molecules, a quantum theory. In: International series of monographs in chemistry, vol 22. Oxford University Press, Oxford
85. Bader RFW, Essen H (1984) J Chem Phys 80:1943
86. Biegler-König F, Schönbohm J, Bayles D (2001) J Comput Chem 22:545
87. Hotta S, Waragai K (1990) In The physics and chemistry of organic superconductors. In: Saito G, Kagoshima S (eds) Springer, Berlin, p 391
88. Abu-Eittah RH, Al-Sugeir FA (1985) Bull Chem Soc Jpn 58:2126
89. Hotta S, Waragai K (1993) J Phys Chem 97:7427
90. Giuffreda MG, Bruschi M, Luethi HP (2004) Chem A Eur J 10:5671
91. Zhan CG, Nichols JA, Dixon DA (2003) J Phys Chem A 107:4184
92. Rienstra-Kiracofe JC, Tschumper GS, Schaefer HF, Nandi S, Ellison GB (2002) Chem Rev 102:231
93. Rienstra-Kiracofe JC, Barden CJ, Brown ST, Schaefer HF (2001) J Phys Chem A 105:524
94. de Oliveira G, Martin JML, de Proft F, Geerlings P (1999) Phys Rev A 60:1034
95. Curtiss LA, Redfern PC, Raghavachari K, Pople JA (1998) J Chem Phys 109:42
96. Mahapatro AK, Ghosh S (2002) Appl Phys Lett 80:4840
97. Chwang AB, Frisbie CD (2000) J Phys Chem B 104:12202
98. Waragai K, Akimichi H, Hotta S, Kano H, Sakaki H (1995) Phys Rev B 52:1786
99. Uchiyama K, Akimichi H, Hotta S, Noge H, Sakaki H (1994) Synth Met 63:57
100. Waragai K, Akimichi H, Hotta S, Kano H, Sakaki H (1993) Synth Met 55–57:4053
101. Hotta S, Waragai K (1993) Adv Mater 5:896
102. Demanze F, Cornil J, Garnier F, Horowitz G, Valat P, Yassar A, Lazzaroni R, Brédas JL (1997) J Phys Chem B 101:4553
103. Hapiot P, Demanze F, Yassar A, Garnier F (1996) J Phys Chem 100:8397
104. Montejo M, Navarro A, Kearley GJ, Vazquez J, Lopez-Gonzalez JJ (2004) J Am Chem Soc 126:15087